

An examination on the direct concentration approach to simulating moisture diffusion in a multi-material system



Dapeng Liu, Jing Wang, Ruiyang Liu, S.B. Park *

Department of Mechanical Engineering, State University of New York at Binghamton, Binghamton, NY 13902–6000, United States

ARTICLE INFO

Article history:

Received 25 October 2015
Received in revised form 12 February 2016
Accepted 10 March 2016
Available online 20 March 2016

Keywords:

Packaging reliability
Moisture diffusion model
Simulation

ABSTRACT

In 2009, Xie et al. proposed a diffusion simulation method called direct concentration approach (DCA), which aimed at solving moisture diffusion problems in electronic packages under a transient temperature environment such as reflow process (“Direct Concentration Approach of Moisture Diffusion and Whole Field Vapor Pressure Modeling for Reflow Process: Part I – Theory and Numerical Implementation,” ASME J. Electron. Packag., 131, p. 031,010). However, our study shows that although the DCA may give reasonably accurate concentration results under several circumstances, its relative error in concentration result can be as high as 10% in one of our test cases. More importantly, the DCA generally leads to the discontinuity of diffusion flux at the bi-material interface, which means that the result may violate the law of mass conservation. A theoretical derivation based on a one-dimensional (1-D) diffusion case is presented to demonstrate the flaw of the DCA using the finite element formulation.

© 2016 Published by Elsevier Ltd.

1. Background

Polymeric packaging materials tend to absorb moisture when they are exposed to a humid environment. Moisture absorbed in the polymer-based materials can have adverse effects on the reliability and integrity of electronic packages by inducing corrosion, hygroscopic stress, popcorn failure, and degradation of the adhesion strength [1–4]. Therefore, it is crucial to evaluate and predict the behavior of moisture diffusion inside the packages, and the finite element method has been adopted by numerous researchers to model moisture diffusion [5–18]. Most researchers have opted to use the Fickian diffusion in their studies. Fick’s first law relates the diffusion flux \mathbf{J} to the gradient of concentration C

$$\mathbf{J} = -D\nabla C \quad (1)$$

where D is the diffusivity, which is generally a function of temperature. In this paper, we assume that all materials are isotropic and D is independent of concentration.

The diffusion process conforms to the law of mass conservation

$$\dot{C} + \nabla \cdot \mathbf{J} = 0. \quad (2)$$

Combining Eqs. (1) and (2) yields the mass diffusion equation

$$\dot{C} = \nabla \cdot (D\nabla C). \quad (3)$$

If the diffusivity is independent of the location, the equation above can be further simplified

$$\dot{C} = D\nabla^2 C. \quad (4)$$

Eq. (3) or Eq. (4) is known as Fick’s second law.

We can find that the governing equation for moisture diffusion is analogous to the governing equation for heat transfer, and the thermal-moisture analogy had been used in previous studies when diffusion capabilities were not supported by most FEA software. However, unlike temperature, which is continuous in nature, moisture concentration is discontinuous across the interface of two dissimilar materials due to the fact that various polymeric materials can have different moisture absorption capabilities (Fig. 1). (See Fig. 2.)

In order to remove the moisture concentration discontinuity at material interfaces, a normalized concentration was introduced [10]

$$\phi = \frac{C}{S}. \quad (5)$$

The normalized concentration is continuous at the bi-material interface according to the Nernst partition rule. By changing the dependent variable from concentration to normalized concentration, commercial finite element software can be utilized to perform the diffusion analysis in a multi-material system.

Wong [11] developed another normalization method using “wetness” or “fractional saturation” w

$$w = \frac{C}{C_{sat}} \quad (6)$$

* Corresponding author.

E-mail address: sbpark@binghamton.edu (S.B. Park).

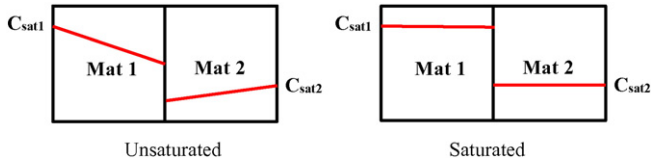


Fig. 1. Moisture concentration discontinuity at bi-material interface.

where C_{sat} is the saturated moisture concentration. C_{sat} is a measure of moisture absorption capacity of the material. The normalized concentration “wetness” is also continuous at material interfaces, which can be proved by the equality principle of chemical potential. These two approaches are mathematically equivalent at a given temperature and humidity because C_{sat} can be expressed according to Henry's law as follows:

$$C_{sat} = SP_{ext} \quad (7)$$

where P_{ext} is the ambient vapor pressure.

Under a constant temperature or humidity case, such as moisture preconditioning, S or C_{sat} does not change with time, and the governing Eq. (3) can be written in terms of ϕ as

$$S\dot{\phi} = \nabla \cdot (DS\nabla\phi). \quad (8)$$

The continuity equation at the material interface requires

$$D_1 S_1 \frac{\partial \phi}{\partial \mathbf{n}} \Big|_{L-} = D_2 S_2 \frac{\partial \phi}{\partial \mathbf{n}} \Big|_{L+} \quad (9)$$

where the subscript numbers denote the material; for example, D_1 represents the diffusivity of Material 1, \mathbf{n} is the normal direction of the interface, and $L-$ and $L+$ denote the two sides, left side and right side in Fig. 1) at the interface L . Eq. (9) can be automatically satisfied for the normalization approach in the finite element method.

Similarly, the governing equation can also be written in terms of w as

$$C_{sat} \dot{w} = \nabla \cdot (DC_{sat} \nabla w). \quad (10)$$

The solubility S is a function of temperature. If the diffusion occurs under a transient thermal environment, the governing equation becomes

$$S\dot{\phi} + \phi\dot{S} = \nabla \cdot (DS\nabla\phi). \quad (11)$$

Similarly, the governing equation in terms of w becomes

$$C_{sat} \dot{w} + w\dot{C}_{sat} = \nabla \cdot (DC_{sat} \nabla w). \quad (12)$$

Solubilities of the materials typically comply with the following form:

$$S = S_0 \exp\left(\frac{E_S}{RT}\right) \quad (13)$$

where S_0 and E_S are material constants. Eq. (13) indicates that it is impossible to drop the second term in Eq. (11) for the diffusion under

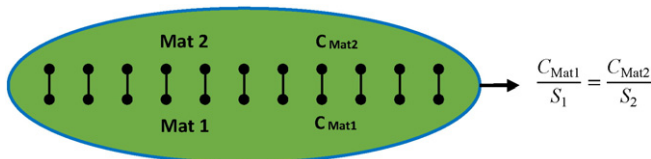


Fig. 2. Coincident nodes and constraint equations at bi-material interface.

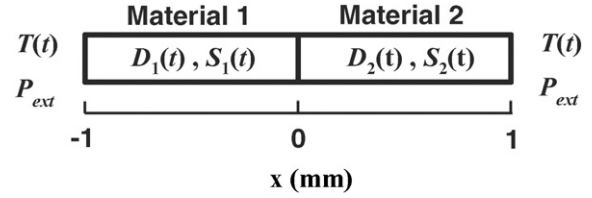


Fig. 3. Geometry and boundary conditions for the case study ($T(t) = 25 + t/60$ °C, $P_{ext} = 3207$ Pa).

the transient thermal condition. However, the effect of \dot{S} is ignored by the FEA software and erroneous results might be obtained [7,15]. As for the normalization method using “wetness”, the definition was ambiguous, because

$$\begin{aligned} C_{sat} &= SP_{ext} = S(P_{sat}\varphi_{RH}) = S\left[P_0 \exp\left(-\frac{E_{VP}}{RT}\right)\varphi_{RH}\right] \\ &= S_0 P_0 \exp\left(\frac{E_S - E_{VP}}{RT}\right)\varphi_{RH} \end{aligned} \quad (14)$$

where P_{sat} is the saturated vapor pressure, φ_{RH} is the relative humidity, E_{VP} is the activation energy for the water vapor, R is the universal gas constant ($8.3145 \text{ J K}^{-1} \text{ mol}^{-1}$), and T is temperature. Paradoxically, numerous studies have shown that at a given relative humidity, there is no strong correlation between the saturated moisture concentration and temperature for many electronic packaging polymers [19], as long as the temperature is much lower than the glass transition temperature (T_g) of the polymers. In other words, $E_S \approx E_{VP}$, and thus C_{sat} is only linearly dependent on humidity. Therefore, $S_0 P_0$ can be treated as a temperature-independent material property, and $C/(S_0 P_0)$ can be used as a new normalized concentration when dealing with transient thermal loading problems in actual simulations, while φ_{RH} can be treated as a boundary condition [14]. This is referred to as the “advanced” normalization method.

Several commercial FEA software packages, such as Abaqus [20] and ANSYS [21], have already offered the capability of diffusion simulation. Besides the Fickian diffusion, Abaqus also provides the general mass diffusion capabilities [20]. In such general mass diffusion model, the diffusion flux \mathbf{J} is driven by a general chemical potential ϕ (normalized concentration or activity of the diffusion material), temperature T , and the equivalent pressure p

$$\mathbf{J} = -SD[\nabla\phi + \kappa_t \nabla \ln(T - T_{Abs0}) + \kappa_p \nabla p] \quad (15)$$

where κ_t is the temperature gradient factor (“Soret” factor), and κ_p is the pressure gradient factor. Clearly, Fick's first law can be considered as a special case of Eq. (15) [9,20]. We discuss only the Fickian diffusion in this paper.

2. Direct concentration approach (DCA)

The experiments showing the temperature-independency of C_{sat} were conducted at relatively low temperatures (under 100 °C). Jang [22] studied the property of the saturated moisture concentration of molding compound under high temperatures, and revealed that C_{sat} increases at temperatures above the T_g . The T_g is material-dependent, the temperature can reach much higher than the T_g of most polymer-based packaging materials during the reflow process, which means C_{sat} cannot be simply treated as a constant. Hence, the aforementioned normalization approaches are not able to accurately simulate the moisture-related issues during reflow process.

In order to solve the moisture diffusion problem under varying ambient temperature conditions, Xie et al. [16] developed the direct concentration approach (DCA). The DCA does not rely on the temperature independence of any material properties, which means it could have a

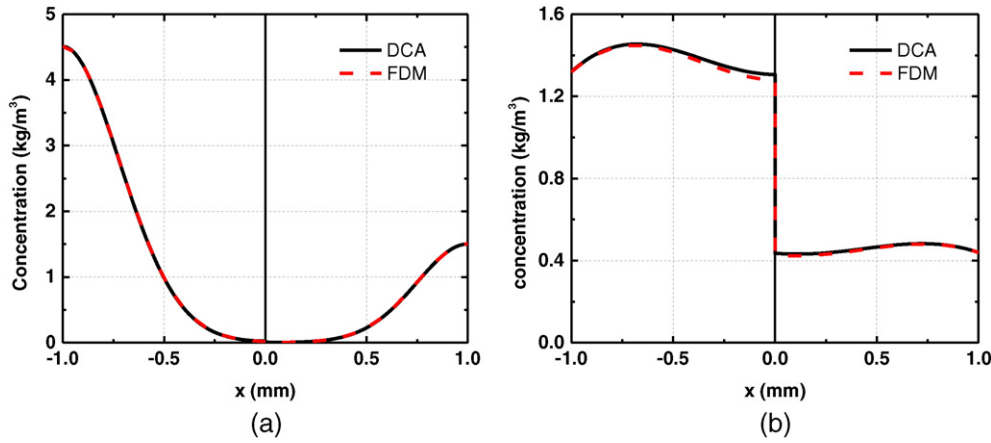


Fig. 4. Moisture concentration in a bi-material specimen subjected to transient thermal loading condition (a) $t = 1800$ s and (b) $t = 3600$ s.

potentially broader field of applications if such an approach were correct.

The direct concentration approach is different from conventional normalization approaches in which the normalized concentration is the field variable. In the DCA, the moisture concentration is directly used as the basic field variable. To represent the discontinuity of moisture concentration, two sets of separate but coincident nodes are built at the bi-material interface. Constraint equations are applied at each pair of the interfacial nodes to “glue” the two materials together to satisfy the continuity relation. The constraint equation is given as

$$\frac{C_{Mat1}}{S_1} = \frac{C_{Mat2}}{S_2} \quad (16)$$

where C_{Mat1} and C_{Mat2} are the moisture concentrations on the bi-material interface, which belong to Material 1 and Material 2, respectively. The authors of Ref. [16] stated that by applying this constraint equation, the continuity of diffusion flux at the interface

$$D_1 \frac{\partial C_{Mat1}}{\partial \mathbf{n}} \Big|_L = D_2 \frac{\partial C_{Mat2}}{\partial \mathbf{n}} \Big|_L \quad (17)$$

would be satisfied automatically.

The researchers who proposed the DCA implemented this approach with ABAQUS to simulate the moisture diffusion and vapor pressure buildup in stacked-die packages during the reflow process [17]. Because the ratio of the saturated concentrations of two materials at the material boundary may not be constant under varying temperatures, the constraint equations need to be updated when this condition applies.

Because such capability is not supported by the commercial FEA software, a new analysis with updated constraint equations needs to be performed when there is a need to update constraint equations.

3. Case studies

3.1. Case 1

Despite the complication of programming brought about by applying and updating the constraint equations (especially when dealing with a three-dimensional model), the DCA appears to be promising due to its independence on the solubility (or the saturated concentration) of the diffusion substance. To examine the DCA, a case study was performed with ANSYS 15.0 to solve the same transient thermal-diffusional problem as in Ref. [14]. The simulation dealt with 1-D diffusion in a bi-material system under the transient thermal loading condition. The geometry of the model is shown in Fig. 3, and the material properties are listed in Table 1. The solubility-temperature relation was assumed to follow Eq. (13) and diffusivities of the materials were assumed to comply with the Arrhenius form

$$D = D_0 \exp\left(-\frac{E_D}{RT}\right) \quad (18)$$

where D_0 is a material constant, and E_D is the activation energy for diffusivity.

In this transient case, the temperature distribution of the bi-material system was uniform in space, but changed with time. The temperature increased at a rate of 1°C per minute from the room temperature

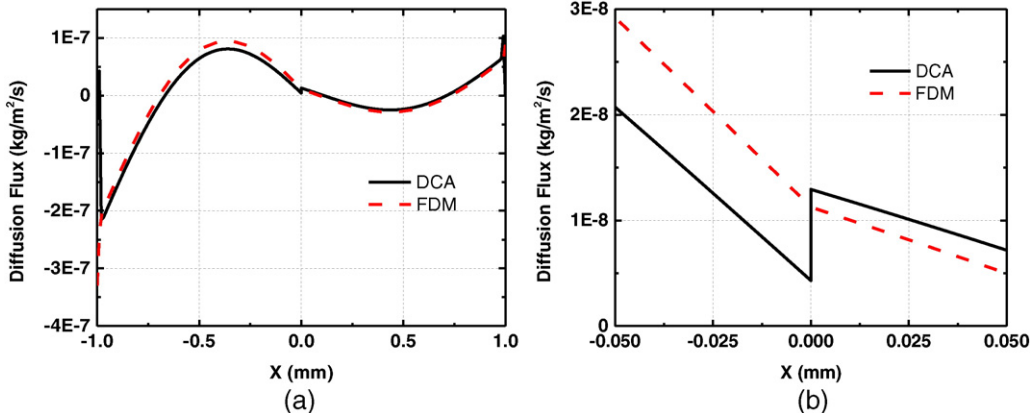


Fig. 5. Diffusion flux distribution at 3600 s (a) full view (b) zoomed view.

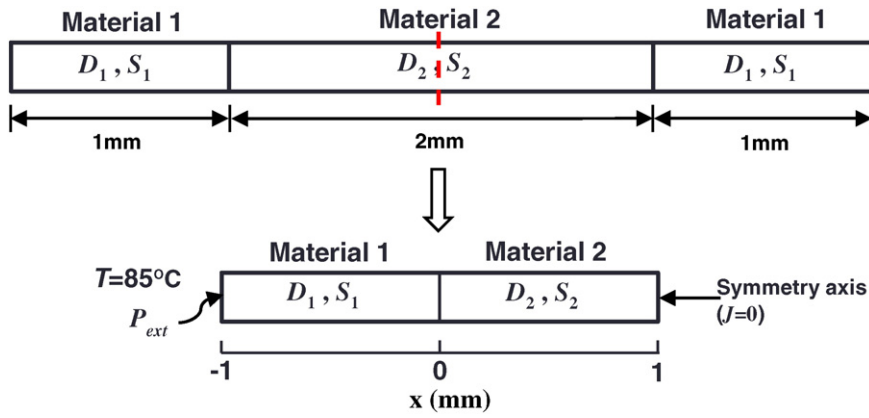


Fig. 6. Sandwich structure (top) and half-symmetry model used in simulation (bottom).

(25 °C), while the ambient vapor pressure was set as 3207 Pa (saturated vapor pressure at 25 °C) and kept constant during the entire process. Moisture diffused simultaneously into the system through the leftmost and rightmost boundaries. The initial moisture concentration in the materials was set to be zero.

An eight-node element for 2-D diffusion analysis (PLANE238) was used for the finite element simulation with ANSYS 15.0. A built-in ANSYS command (CE), which applies constraint equations onto the interfacial nodes, was used to implement Eq. (16) as required by the DCA. During the calculation, the constraint equation remained unchanged because the ratio of solubility of two materials (S_1/S_2) was a constant. We used the same element size as in Refs. [14,15]. There were 200 elements through the thickness of each slab (mapped mesh with element size of $0.005 \text{ mm} \times 0.005 \text{ mm}$).

Fig. 4 shows the distributions of moisture concentration along x -direction at 1800 s and 3600 s. We also included numerical results based on the finite difference method (FDM) for comparison. The FDM results were previously published in Ref. [14,15] and agreed with the solutions obtained from advanced normalized approach (not shown in Fig. 4). The forward-time central-space (FTCS) method was used in the FDM program, and Eq. (9) was utilized at the material interface for ensuring a continuous mass flux. Ref. [7] described the algorithm for this particular problem.¹

It can be seen that the DCA yields slightly larger results than the FDM at 3600 s. Intuitively, this difference can be easily treated as numerical error. However, this small amount of difference is not due to the numerical error and cannot be eliminated. More importantly, a closer check of the diffusion flux result (Fig. 5) shows that the diffusion flux is discontinuous across the bi-material interface, which violates the law of mass conservation. Actually, the ratio of the diffusion flux at the interface of Material 1 and Material 2 equals 1/3, which is the inverse of the ratio of the solubility (S_1/S_2).

3.2. Case 2

Frankly speaking, this case is not illustrative enough to demonstrate the feasibility of DCA, because the amount of diffusion flux through the bi-material interface is quite limited.

Therefore, we performed another simulation to examine the results generated by the DCA. Our guidelines for designing this test case are as follows:

1. A constant-temperature environment should be applied. On the one hand, it eliminates the potential numerical error due to exponentially

changing the material properties; on the other hand, it allows us to determine whether the discontinuity issue is due to the transient thermal condition.

2. Try to use the same material properties, geometry, mesh, and constraint equations as in Case 1. Hence we do not need to rebuild the geometry and need only to change the boundary conditions.
3. The moisture diffusion flux at the material interface should be increased.
4. The boundary conditions must be practical, i.e., Eq. (14) must be satisfied so that we cannot set an arbitrary concentration value as the boundary condition.

In the second case, we considered a sandwich structure with two materials (Fig. 6). The leftmost and rightmost portions are made of the same material while the middle part is made of another material. Assume that the lengths of the left, middle, and right portions are 1 mm, 2 mm, and 1 mm, respectively, and the moisture ingresses into the assembly from both leftmost and rightmost boundaries (top and bottom boundaries are moisture-insulated) under constant temperature at 85 °C. Owing to the symmetry, this model can be simplified to a half-symmetry model shown in Fig. 6, which includes only the left half of the sandwich structure. In the half-symmetry model, the moisture diffuses into the material only from the leftmost boundary, and the diffusion flux of the symmetry boundary is set as zero.

In this case, moisture absorbed by Material 1 needs to travel through the material interface for diffusing into Material 2; thus, it is suitable to

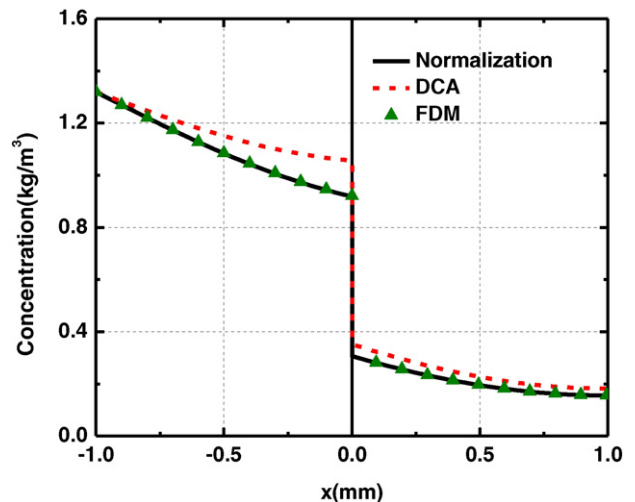


Fig. 7. Moisture concentration distribution along the x -axis at 3600 s.

¹ Please note that there is a typo in Eq. (A6) in Ref. [7]. The subscript $L + \Delta x$ should be $L - \Delta x$, and the $L - \Delta x$ should be $L + \Delta x$.

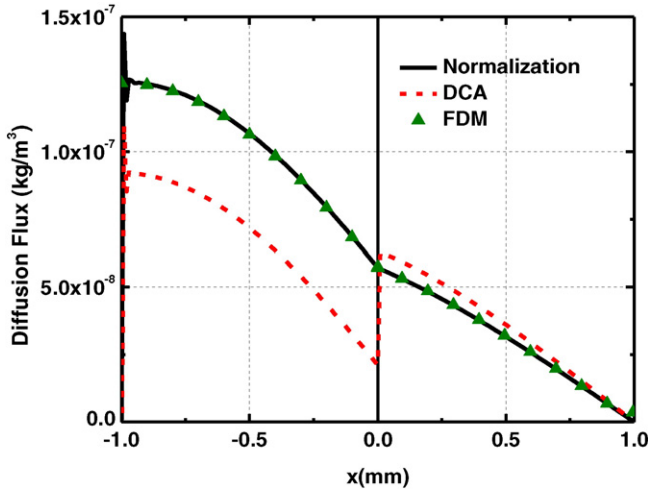


Fig. 8. Diffusion flux distribution along the x-axis at 3600 s.

show the difference. This case was performed using the DCA and the normalization approach in ANSYS. The ambient vapor pressure remained the same as in Case 1. The finite difference method was again adopted as the reference. Figs. 7 and 8 plot the results of moisture concentration and diffusion flux at 3600 s, respectively. It is obvious that the concentration result of the DCA deviates distinctively from the reference result. Moreover, the diffusion flux obtained by the DCA is discontinuous at the material interface, which indicates that the DCA result was a wrong solution.

4. Discussions

The authors who proposed the DCA claimed that the continuity for diffusion flux at the material interface “will automatically be satisfied through the finite element formulation,” “according to the variational principle” by establishing constraint equations. However, according to the results of above case studies, such flux continuity cannot be satisfied by merely establishing the constraint equations at the interface. In this part, a theoretical derivation based on a simple geometry is used to find out the root cause of this flaw.

The discontinuity of diffusion flux using DCA happens during the implementation of the constraint equations, which can be proved by the theory of finite element method. In this study, one-dimensional (1-D) diffusion in a bi-material model with bar elements is considered (Fig. 9). Constant moisture concentrations are applied at the leftmost and rightmost boundaries, and the initial concentration of the system is zero. The diffusivities and saturated moisture concentrations of the two materials are different. The ratio of saturated moisture concentration of the two materials (C_{sat1}/C_{sat2}) is a constant. Assume both Material 1 and Material 2 have two elements, and the length of each element is the same. In order to perform the DCA, two coincident nodes (Node 3

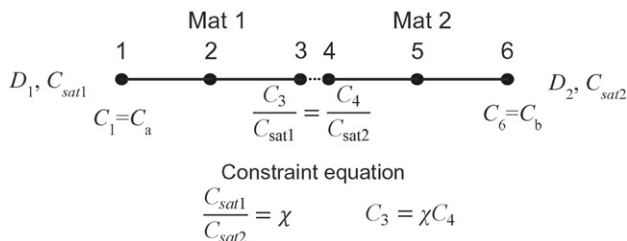


Fig. 9. Geometry and boundary conditions for the finite element analysis.

Table 1
Material properties used in the simulation.

	Material 1	Material 2
$D_0(\text{m}^2 \text{s}^{-1})$	5×10^{-3}	4×10^{-3}
$S_0(\text{kg m}^{-3} \text{Pa}^{-1})$	6×10^{-10}	2×10^{-10}
$E_p(\text{J mol}^{-1})$	5×10^4	5×10^4
$E_s(\text{J mol}^{-1})$	4×10^4	4×10^4

and Node 4) are generated at the bi-material interface. The shape function for each element is [23]

$$\{N\} = \left[1 - \frac{x}{h} \quad \frac{x}{h} \right]^T \quad (19)$$

where h is the length of the 1-D bar element. Therefore, the concentration over the element can be expressed as

$$C = \{N\}^T \{C_e\} \quad (20)$$

where $\{C_e\}$ is the nodal concentration vector. The governing equation of the diffusion process can be expressed as

$$[K^d] \{C_e\} + [C^d] \{\dot{C}_e\} = \{R_e\} \quad (21)$$

where $[K^d]$ is the diffusion conductivity matrix, $[C^d]$ is the diffusion damping matrix, and $\{R_e\}$ represents the combination of element diffusion flux, applied flow rate, and generation of diffusion substances in an element [21]. If the normalized concentration is used, the diffusion conductivity matrix can be expressed as

$$[K^d] = C_{sat} \int_0^h (\nabla \{N\}^T)^T [D] (\nabla \{N\}^T) dx \quad (22)$$

where $[D]$ is the diffusivity matrix. For this 1-D diffusion problem, $[D] = D$. The element diffusion damping matrix is

$$[C^d] = C_{sat} \int_0^h \{N\} \{N\}^T dx. \quad (23)$$

The value of C_{sat} will be assigned as 1 if the DCA is used. In this case, for 1-D two-node element, the local diffusion conductivity matrix and diffusion damping matrix can be expressed as

$$[K^d] = \frac{1}{h} \begin{bmatrix} D & -D \\ -D & D \end{bmatrix} \quad (24)$$

$$[C^d] = \frac{h}{6} \begin{bmatrix} 2 & 1 \\ 1 & 2 \end{bmatrix}. \quad (25)$$

Therefore, the global diffusion conductivity matrix and the global diffusion damping matrix become the following form after the assembly process:

$$[K^d] = \frac{1}{h} \begin{bmatrix} D_1 & -D_1 & 0 & 0 & 0 & 0 \\ -D_1 & 2D_1 & -D_1 & 0 & 0 & 0 \\ 0 & -D_1 & D_1 & 0 & 0 & 0 \\ 0 & 0 & 0 & D_2 & -D_2 & 0 \\ 0 & 0 & 0 & -D_2 & 2D_2 & -D_2 \\ 0 & 0 & 0 & 0 & -D_2 & D_2 \end{bmatrix} \quad (26)$$

$$[C^d] = \frac{h}{6} \begin{bmatrix} 2 & 1 & 0 & 0 & 0 & 0 \\ 1 & 4 & 1 & 0 & 0 & 0 \\ 0 & 1 & 2 & 0 & 0 & 0 \\ 0 & 0 & 0 & 2 & 1 & 0 \\ 0 & 0 & 0 & 1 & 4 & 1 \\ 0 & 0 & 0 & 0 & 1 & 2 \end{bmatrix}. \quad (27)$$

As for $\{R_e\} = \{R_1 \dots R_6\}^T$, the boundary condition is applied at Node 1 and Node 6, so R_1 and R_6 are unknown (need to be calculated), while R_2, R_3, R_4 and R_5 are zero.

In the DCA, the constraint equation is applied at interface nodes as

$$C_3 = \chi C_4 \quad (28)$$

where χ is the ratio of $C_{\text{sat}1}$ and $C_{\text{sat}2}$ ($\chi \neq 1$). There are three ways to implement the constraint equation in FEM; namely, the master–slave elimination, the penalty augmentation, and Lagrange multiplier adjunction [24]. In this paper, the master–slave elimination method is used, in which the degree-of-freedom (DOF) to be eliminated is the slave DOF, and the remaining one is the master DOF. Therefore, a new set of DOFs $\{\widehat{C}_e\}$ can be obtained after eliminating the slave DOF. The relationship between the old and new sets of DOF can be established with the transformation matrix [T]

$$\{C_e\} = [T]\{\widehat{C}_e\}. \quad (29)$$

In this case, C_3 is chosen as the slave DOF, while C_4 is the master DOF; Eq. (29) can be expressed in the following form:

$$\begin{Bmatrix} C_1 \\ C_2 \\ C_3 \\ C_4 \\ C_5 \\ C_6 \end{Bmatrix} = \begin{bmatrix} 1 & 0 & 0 & 0 & 0 \\ 0 & 1 & 0 & 0 & 0 \\ 0 & 0 & \chi & 0 & 0 \\ 0 & 0 & 1 & 0 & 0 \\ 0 & 0 & 0 & 1 & 0 \\ 0 & 0 & 0 & 0 & 1 \end{bmatrix} \begin{Bmatrix} \widehat{C}_1 \\ \widehat{C}_2 \\ \widehat{C}_4 \\ \widehat{C}_5 \\ \widehat{C}_6 \end{Bmatrix}. \quad (30)$$

Because the value of χ remains constant in the finite element analysis and $C_3 = \chi C_4$ is always satisfied, it is easy to find $\widehat{C}_3 = \chi \widehat{C}_4$. Therefore, the same transformation matrix also relates to the derivative matrix

$$\{\dot{C}_e\} = [T]\{\dot{\widehat{C}}_e\}. \quad (31)$$

Substituting Eqs. (29) and (31) into Eq. (21), and pre-multiplied by $[T]^T$ on both sides, gives

$$[T]^T [K^d] [T] \{C_e\} + [T]^T [C^d] [T] \{\dot{C}_e\} = [T]^T \{R_e\}. \quad (32)$$

Letting $[\widehat{K}^d] = [T]^T [K^d] [T]$, $[\widehat{C}^d] = [T]^T [C^d] [T]$ and $[\widehat{R}_e] = [T]^T \{R_e\}$, Eq. (32) becomes

$$[\widehat{K}^d] \{\widehat{C}_e\} + [\widehat{C}^d] \{\dot{\widehat{C}}_e\} = \{\widehat{R}_e\}. \quad (33)$$

As for the vector $\{R_e\}$, because both R_3 and R_4 are zero, and the transformation removes only one zero, so $\{\widehat{R}_e\} = \{R_1 \ 0 \ 0 \ 0 \ R_6\}^T$. Therefore, the complete expression of the new governing equation becomes

$$\frac{1}{h} \begin{bmatrix} D_1 & -D_1 & 0 & 0 & 0 \\ -D_1 & 2D_1 & -\chi D_1 & 0 & 0 \\ 0 & -\chi D_1 & \chi^2 D_1 + D_2 & -D_2 & 0 \\ 0 & 0 & -D_2 & 2D_2 & -D_2 \\ 0 & 0 & 0 & -D_2 & D_2 \end{bmatrix} \begin{Bmatrix} \widehat{C}_1 \\ \widehat{C}_2 \\ \widehat{C}_4 \\ \widehat{C}_5 \\ \widehat{C}_6 \end{Bmatrix} + \frac{h}{6} \begin{bmatrix} 2 & 1 & 0 & 0 & 0 \\ 1 & 4 & \chi & 0 & 0 \\ 0 & \chi & 2\chi^2 + 2 & 1 & 0 \\ 0 & 0 & 1 & 4 & 1 \\ 0 & 0 & 0 & 1 & 2 \end{bmatrix} \begin{Bmatrix} \dot{\widehat{C}}_1 \\ \dot{\widehat{C}}_2 \\ \dot{\widehat{C}}_4 \\ \dot{\widehat{C}}_5 \\ \dot{\widehat{C}}_6 \end{Bmatrix} = \begin{Bmatrix} R_1 \\ 0 \\ 0 \\ 0 \\ R_6 \end{Bmatrix}. \quad (34)$$

If we consider only the third row and expand the equation, substituting χC_4 with C_3 , and re-arranging the items yields

$$-\chi \left(D_1 \frac{C_3 - C_2}{h} + \frac{h}{6} (\dot{C}_2 + 2\dot{C}_3) \right) = -D_2 \frac{C_5 - C_4}{h} + \frac{h}{6} (\dot{C}_5 + 2\dot{C}_4). \quad (35)$$

The left-hand side of Eq. (35) equals to J_1 , and the right-hand side equals to J_2 , where J_1 is the diffusion flux at the interface on Material 1 side and J_2 is the diffusion flux at the interface on Material 2 side. The relationship of

$$\chi J_1 = J_2 \quad (36)$$

is always true if the DCA is used. Thus, DCA violates the rule of mass conservation unless

$$\chi = 1 \quad (37)$$

or

$$J_1 = J_2 = 0. \quad (38)$$

As for the verification case in Ref. [16], Material 2 is essentially not permeable to moisture. At the beginning of the desorption process, the amount of moisture in Material 2 is only 0.03% of the whole system. Hence, the flux through the material interface is extremely small, and the flux discontinuity issue will not have distinctive effect on the average concentration of the system. Therefore, it is reasonable to say that Eq. (38) is satisfied so that the DCA is valid in such situation. This can be confirmed by the analytical solution [16]. Plus, the seemingly good agreement between the concentration distribution curves in Fig. 4 is also due to the low diffusion flux at the interface, especially for subplot (a) at 1800 s.

For the second case in this paper, the difference between the results of FDM and DCA is obvious due to larger diffusion flux through the interface than that in the previous case. Because the first-type boundary condition (fixed-value boundary condition or Dirichlet boundary condition) is used in our simulation cases, the data points to the exterior boundaries should always match. Readers may perform extra cases to examine the effects of dimensions and material properties. We will not conduct comprehensive quantitative analysis on the simulation error of the DCA in this paper, because several new methods are available [18,25]. For example, a convection–diffusion porous media model has been proposed for moisture transport at high temperatures, and this model also considers the non-Fickian behavior by adopting the concept of dual-stage model [25]. Furthermore, researches are typically more concerned about the consequence of moisture. Several researchers have worked on integrated stress analysis that combines the thermomechanical stress with the moisture-induced stresses in electronic packages. For example, Fan and Zhao applied thermal expansion, hygroscopic swelling and vapor pressure simultaneously in their simulation [9]. Yoon et al. included nonlinear material properties together with the thermal expansion and the hygroscopic swelling behavior [12]. Kim et al. included the shift effect of T_g caused by moisture absorption into the viscoelastic stress analysis [13]. Liu discussed the numerical implementation methodology of this T_g -shift effect [26].

5. Summary

We observed the discontinuity of diffusion flux at the bi-material interface when we tried to implement the direct concentration approach in a finite element simulation. Then another test case was created to achieve more evident discontinuity in diffusion flux. Finally, we utilized the theories of finite element formulation and multi-freedom constraint to find out the root cause of this flux-discontinuity phenomenon caused by the DCA. Results have proved that such discontinuity is due to the implementation of constraint equations, and this discontinuity is

independent of temperature profiles. As a conclusion, the direct concentration approach is flawed. The DCA can yield correct results only when the saturated moisture concentrations of the materials are identical, or the diffusion flux across the bi-material interface is negligible, which renders this approach inappropriate for general cases.

Acknowledgement

The authors would like to thank all members of Opto-Mechanics and Physical Reliability Lab at SUNY-Binghamton for their intelligent support during this study.

References

- [1] M. Kitano, A. Nishimura, S. Kawai, Analysis of package cracking during reflow soldering process, IRPS Conf. (1998) 90–95.
- [2] E.H. Wong, R. Rajoo, S.W. Koh, T.B. Lim, The mechanics and impact of hygroscopic swelling of polymeric materials in electronic packaging, *J. Electron. Packag.* 124 (2002) 122–126.
- [3] X. Fan, G. Zhang, W.D. van Driel, L.J. Ernst, Interfacial delamination mechanisms during soldering reflow with moisture preconditioning, *IEEE Trans. Components Packag. Technol.* 31 (2008) 252–259.
- [4] X. Fan, Mechanics of moisture for polymers: fundamental concepts and model study, thermal, mechanical and multi-physics simulation and experiments in microelectronics and micro-systems, 2008, EuroSimE 2008. International Conference on 2008, pp. 1–14.
- [5] A.A.O. Tay, L. Tingyu, Moisture diffusion and heat transfer in plastic IC packages, *Components Packag. Manuf. Technol. A IEEE Trans.* 19 (1996) 186–193.
- [6] E. Wong, S. Koh, K. Lee, R. Rajoo, Advanced moisture diffusion modeling and characterisation for electronic packaging, electronic components and technology conference, 2002, Proceedings. 52nd, IEEE 2002, pp. 1297–1303.
- [7] S. Yoon, B. Han, Z. Wang, On moisture diffusion modeling using thermal-moisture analogy, *J. Electron. Packag.* 129 (2007) 421–426.
- [8] J.B. Kwak, S. Park, Integrated hygro-swelling and thermo-mechanical behavior of mold compound for MEMS package during reflow after moisture preconditioning, *Microelectron. Int.* 32 (2015) 8–17.
- [9] X. Fan, J.-H. Zhao, Moisture diffusion and integrated stress analysis in encapsulated microelectronics devices, 12th International Conference on Thermal, Mechanical and Multi-Physics Simulation and Experiments in Microelectronics and Microsystems (EuroSimE) 2011, pp. 1/8–8/8.
- [10] J.E. Galloway, B.M. Miles, Moisture absorption and desorption predictions for plastic ball grid array packages, *IEEE Trans. Components Packag. Manuf. Technol. A* 20 (1997) 274–279.
- [11] E.H. Wong, Y.C. Teo, T.B. Lim, Moisture diffusion and vapour pressure modeling of IC packaging, electronic components & technology conference, 1998, 48th IEEE, IEEE 1998, pp. 1372–1378.
- [12] S. Yoon, C. Jang, B. Han, Nonlinear stress modeling scheme to analyze semiconductor packages subjected to combined thermal and hygroscopic loading, *J. Electron. Packag.* 130 (2008) 024502.
- [13] Y. Kim, D. Liu, H. Lee, R. Liu, D. Sengupta, S. Park, Investigation of stress in MEMS sensor device due to hygroscopic and viscoelastic behavior of molding compound, *IEEE Trans. Components Packag. Manuf. Technol.* 5 (2015) 945–955.
- [14] C. Jang, S. Park, B. Han, S. Yoon, Advanced thermal-moisture analogy scheme for anisothermal moisture diffusion problem, *J. Electron. Packag.* 130 (2008) 011004.
- [15] D. Liu, S. Park, A note on the normalized approach to simulating moisture diffusion in a multmaterial system under transient thermal conditions using ansys 14 and 14.5, *J. Electron. Packag.* 136 (2014) 034501.
- [16] B. Xie, X.J. Fan, X.Q. Shi, H. Ding, Direct concentration approach of moisture diffusion and whole-field vapor pressure modeling for reflow process – part I: theory and numerical implementation, *J. Electron. Packag.* 131 (2009) 031010.
- [17] B. Xie, X.J. Fan, X.Q. Shi, H. Ding, Direct concentration approach of moisture diffusion and whole-field vapor pressure modeling for reflow process—part II: application to 3D ultrathin stacked-die chip scale packages, *J. Electron. Packag.* 131 (2009) 031011.
- [18] E. Wong, The fundamentals of thermal-mass diffusion analogy, *Microelectron. Reliab.* 55 (2015) 588–595.
- [19] E.H. Wong, R. Rajoo, Moisture absorption and diffusion characterization of packaging materials – advanced treatment, *Microelectron. Reliab.* 43 (2003) 2087–2096.
- [20] Dassault Systemes, Mass Diffusion Analysis, Analysis User's Manual, 2010.
- [21] ANSYS, Inc., ANSYS Mechanical APDL Theory Reference, Release 14.5, Canonsburg, PA, 2013.
- [22] C. Jang, B. Han, S. Yoon, Comprehensive moisture diffusion characteristics of epoxy molding compounds Over Solder Reflow process temperature, *IEEE Trans. Components Packag. Technol.* 33 (2010) 809–818.
- [23] J.N. Reddy, An Introduction to the Finite Element Method, third ed. McGraw-Hill, New York, 2006.
- [24] C. Felippa, MultiFreedom Constraints I, Introduction to Finite Element Methods, University of Colorado at Boulder, 2015.
- [25] L. Chen, H.W. Chu, X. Fan, A convection-diffusion porous media model for moisture transport in polymer composites: model development and validation, *J. Polym. Sci. B Polym. Phys.* 53 (2015) 1440–1449.
- [26] D. Liu, Packaging-Induced Stresses on Microelectromechanical Systems, Mechanical Engineering, State University of New York at Binghamton, Binghamton, NY, 2015.